Pharm Res (2015) 32:3087–3101
DOI 10.1007/s11095-015-1689-z

RESEARCH PAPER

In Vitro and *In Vivo* Efficacy of Self-Assembling RGD Peptide Amphiphiles for Targeted Delivery of Paclitaxel

Poonam Saraf[1] • Xiaoling Li[1] • Lisa Wrischnik[2] • Bhaskara Jasti[1]

Received: 30 December 2014 / Accepted: 26 March 2015 / Published online: 11 June 2015

ABSTRACT

Purpose The objective of this work was to compare the efficacy of self-assembling cyclic and linear RGD peptide amphiphiles as carriers for delivering paclitaxel to $\alpha_v\beta_3$ integrin overexpressing tumors.

Methods Linear (C18-ADA5-RGD) and cyclic (C18-ADA5-cRGDfK) peptide amphiphiles were synthesized and characterized for CMC, aggregation number and micelle stability using fluorescence spectroscopy methods. Size and morphology of micelles was studied using TEM. Fluorescence polarization and confocal microscopy assays were established to compare binding and internalization of micelles. The targeting efficacy was studied in A2058 cells using cytotoxicity assay as well as *in vivo* in melanoma xenograft mouse model.

Results The linear and cyclic RGD amphiphiles exhibited CMC of 25 and 8 μM, respectively, formed nano-sized spherical micelles and showed competitive binding to $\alpha_v\beta_3$ integrin protein. FITC-loaded RGD micelles rapidly internalized into A2058 melanoma cells. Paclitaxel-loaded RGD micelles exhibited higher cytotoxicity compared with free drug in A2058 cells *in vitro* as well as *in vivo*.

Conclusion Cyclic RGD micelles exhibited better targeting efficacy but were less effective compared to linear RGD micelles as drug delivery vehicle due to lower drug solubilization capacity and lesser kinetic stability. Results from the study proved the effectiveness of self-assembling low molecular weight RGD amphiphiles as carriers for targeted delivery of paclitaxel.

Electronic supplementary material The online version of this article (doi:10.1007/s11095-015-1689-z) contains supplementary material, which is available to authorized users.

✉ Bhaskara Jasti
bjasti@pacific.edu

[1] Department of Pharmaceutics and Medicinal Chemistry, Thomas J. Long School of Pharmacy and Health Sciences, University of the Pacific, Stockton, USA

[2] Department of Biology, College of the Pacific, University of the Pacific, Stockton, USA

KEY WORDS micelles · paclitaxel · RGD · self-assembly · targeting

ABBREVIATIONS

C16 (in amphiphile structures)	Palmitic acid
C18 (in amphiphile structures)	Stearic acid
ADA	8-amino-3,6-dioxaoctanoic acid
HOBT	Hydroxybenzotriazole
HATU	2-(1H-7-azabenzotriazol-1-yl) -1,1,3,3-tetramethyl uronium hexafluorophosphate
PyBOP	Benzotriazol-1-yl-oxytripyrrolidinophosphonium hexafluorophosphate
DIPEA	N, N′-Diisopropylethylamine
DIC	N, N′-Diisopropylcarbodiimide
DCM	Dichloromethane
DMF	N,N′-dimethyl formamide
TFA	Trifluoroacetic acid
TIS	Triisopropylsilane
MALDI-TOF	Matrix assisted laser desorption/ ionization-time of flight
CMC	Critical micellization concentration
N_{agg}	Aggregation number
TEM	Transmission electron microscopy
κ	Molar solubilization capacity
FRET	Forster resonance energy transfer
DII	1,1′-dioctadecyl-3,3,3,3′, Tetramethylindocarbocyanine perchlorate

DIO	3,3′-dioctadecyloxacarbocyanine perchlorate
FP	Fluorescence polarization
mP	Milli polarization units
FITC	Fluorescein isothiocynate
IACUC	Institutional animal care and use committee

INTRODUCTION

The cytotoxicity of anticancer drugs to normal cells in the body causes severe side-effects in patients undergoing chemotherapy and consequently have a negative impact on health and well-being of cancer patients [1]. Targeting of drugs directly to tumors is a strategy for achieving enhanced efficacy and minimizing unwanted toxicity [2]. The products developed and approved so far for the hydrophobic chemotherapeutic drug paclitaxel include *Taxol* and *Abraxane. Taxol* is a micellar form of paclitaxel, which exhibits non-specific cytotoxic effect on the cells and has toxic side effects arising from the Cremophor EL vehicle as well [3]. *Abraxane*—the injectable suspension of albumin-bound paclitaxel—shows limited clinical benefits with respect to cancer patient survival rate; a shortcoming most probably attributed to the large size (130 nm) of the carrier resulting in ineffective tumor penetration [4]. Thus, there is still an unmet need for developing a drug delivery system that will specifically target and internalize its contents into the tumor cells. This can be achieved by designing a nanoparticulate system that can facilitate specific binding or interaction with the tumor cells.

The $\alpha_v\beta_3$ integrin proteins are overexpressed in a variety of tumors including melanoma and this characteristic feature can be exploited for active targeting and delivery of chemotherapeutic drugs to tumors [5]. Studies based on interaction of $\alpha_v\beta_3$ integrin with its endogenous ligands such as vitronectin and fibronectin have revealed that the Arg-Gly-Asp (RGD) sequence is important for integrin recognition [6], and cyclic RGD, which has an improved conformational stability than its linear counterpart, can potentially inhibit the binding of ligands to integrin [7]. Although RGD peptides were unable to clear the clinical trials, they have tremendous potential as ligands for target recognition [8].

Multivalency describes the event of multiple molecular interaction of the same kind between two entities and is a useful approach for enhancing ligand binding affinity. Non-covalent multivalent ligands consist of multiple recognition units and their binding to the target is stabilized by non-covalent interactions. Self-assembly is a useful strategy for designing and presenting ligands with multiple binding sites to receptors for recognition and binding. The tight binding of multivalent ligands to a receptor can be explained by considering the combined effect of affinity and avidity. The avidity of a multivalent system is more than a mere sum of affinities since multivalent ligands can improve ligand binding through various mechanisms [9]. For instance, in a multivalent system, the high concentration of ligands can increase the chances of the ligand rebinding to the receptor after dissociation. Additionally, the binding of multivalent ligands may be favored entropically. Especially, the integrin receptor is considered as a favorable receptor for multiple-ligand binding since it is present in clusters on the cell surface [10].

The multivalent interaction of RGD ligands with integrin receptors have been achieved mostly through covalent conjugation of RGD peptide on the surface of polymers (e.g., polymeric nanoparticles or polymeric micelles) [11–14]. More recently, peptide amphiphiles composed of hydrophilic and hydrophobic sequences of amino acids have found favorable applications in drug delivery and tissue engineering. The peptide amphiphiles can self-assemble into nanostructures ranging from spherical micelles to nanofibers. The design of such peptide amphiphiles plays a crucial role in determining the structure of the self-assembled nanocarriers. Certain designs can favor distinct secondary structures and eventually lead to the formation of cylindrical and fibrous self-assemblies [15–17]. We have previously reported the synthesis and self-assembly of fatty acid conjugated RGD peptide amphiphiles into nanostructures with the potential to deliver paclitaxel selectively into tumor cells overexpressing integrin receptors [18, 19]. The major limitation of the amphiphiles previously studied was their aqueous solubility and higher particle size. Incorporation of 1 or 2 units of flexible hydrophilic linker in the structure of the fatty acid RGD conjugates (C16-ADA-RGD, C18-ADA2-RGD, C16-ADA2RGD, C18-ADA2-RGD) resulted into a limited improvement in solubility of the amphiphiles and lowered their CMC in comparison to the amphiphiles which were direct conjugates of fatty acid and RGD (C18-RGD and C16-RGD). For micellar systems, since the drug loading is a linear function of amphiphile concentration; higher aqueous solubility of the amphiphiles will also improve their drug loading capacity. Therefore the first objective of the present study was to enhance the aqueous solubility of the previously synthesized linear RGD amphiphiles by increasing the chain length of the hydrophilic ADA linker from 2 units to 5 units. The cyclic RGD peptide has better conformational stability and better binding affinity compared to the linear peptide, the second aim of the study was to synthesize amphiphiles of cyclic RGD and compare their drug delivery efficacy with the linear RGD amphiphiles. In the present study, linear and cyclic RGD peptide amphiphiles (C18-ADA5-RGD and C18-ADA5-cRGDfK), respectively, were synthesized using standard solid phase peptide synthesis protocol and the conjugation of stearic acid to the peptides was achieved via multiple units of flexible, hydrophilic 8-amino3,6-dioxaoctanoic acid (ADA) linkers. After

characterizing the self-assembly and physicochemical properties of the micelles, the ability of the micelles to deliver paclitaxel effectively into $\alpha_v\beta_3$ integrin overexpressing melanomas was assessed experimentally in vitro, in cell based model and *in vivo*, in the mouse xenograft model.

MATERIALS AND METHODS

Materials

The Wang resin preloaded with Fmoc-Asp (OtBu)-OH, 2-chloro trityl chloride resin (100–200 mesh), and piperidine were purchased from Advanced Chemtech (Louisville, KY, USA). All peptide synthesis reagents including amino acids (Fmoc-Gly-OH, Fmoc-Arg(Pbf)-OH, Fmoc-Phe-OH, Fmoc-Lys-Dde, Triisopropylsilane (TIS), *N*-hydroxybenzotriazole (HOBT), 2-(1H-7-azabenzotriazol-1-yl)-1,1,3,3-tetramethyluronium hexafluorophosphate (HATU), 8-amino-3,6-dioxaoctanoic acid (ADA) and benzotriazol-1-yl-oxytripyrrolidinophosphonium hexafluorophosphate(PyBOP) were purchased from Chemimpex (Chicago, IL, USA). Stearic acid, Diethyl ether, trifluoroacetic acid (TFA), N, N′-Diisopropylethylamine (DIPEA), N, N′-Diisopropylcarbodiimide (DIC), Triisopropylsilane (TIS), and Tetrakis(triphenylphosphine) palladium were obtained from Acros organics (NJ, USA). Solvents used including dichloromethane (DCM), N,N′-dimethyl formamide (DMF), methanol, acetonitrile were of HPLC grade purchased from Fisher Scientific (PA, USA). Castor Oil Ethoxylated (Cremophor EL) was purchased from Spectrum Chemicals. Copper for transmission electron microscopy (TEM) was purchased from Ted Pella Inc (CA, USA). Dialysis membrane was purchased from Spectrum Labs (CA, USA). Paclitaxel was purchased from LC laboratories (MA, USA). The human $\alpha_v\beta_3$ integrin protein (formulated in Triton X-100) was purchased from Millipore (MA, USA). The fluorescent cyclic RGD probes Cyclo[−RGDy-K(5-FAM)] and cyclo (−RGDfK) were purchased from AnaSpec (CA, USA). Fluorescein isothiocynate (FITC) was purchased from Calbiochem (San Diego, CA, USA). Cell culture reagents including Dulbecco's modified Eagle's medium (DMEM), L-Glutamine, Trypsin (TrypLE Express), Hanks Balanced Salt Solution (HBSS), recovery cell culture freezing media, Alexa fluor 594 wheat germ agglutinin, slow fade gold mounting medium and FRET dyes, namely, 1,1′-dioctadecyl-3,3,3,3′-tetramethylindocarbocyanine perchlorate (DiI) and 3,3′-dioctadecyloxacarbocyanine perchlorate (DiO) were purchased from Invitrogen (CA, USA). SRB assay reagents were purchased from Sigma Aldrich (USA). A2058 and Detroit 551 cell lines were purchased from ATCC (VA, USA). Four to five week old athymic nude (homozygous) (nu/nu) mice were purchased from Simonsen Laboratories (CA, USA).

Design and Synthesis of RGD Peptide Amphiphiles

The interaction of cyclic and linear RGD peptide ligands with alpha v beta 3 integrin receptor were studied using Molecular Operating Environment software (Details in Supplementary Material). The peptide amphiphiles were synthesized by following standard solid phase peptide synthesis procedure. The cyclic RGD amphiphile (C18-ADA5-cRGDfK) was synthesized entirely on solid support. Several protocols for synthesis of the cyclic RGD (cRGDfV or cRGDfK) peptide have been reported and modified for improved yields. The cyclic RGD peptide was built on solid phase using the protocol reported by McCusker *et al.* with some modifications [20]. The O-allyl protected aspartic acid, Fmoc-Asp-OAll (2.5 equivalents) was loaded on the 2-chloro trityl chloride resin in the presence of 10 equivalents of N,N-diisopropylethylamine (DIPEA) for 5 h. After washing the resin with DMF (3 times) and DCM (3 times), the amino group was deprotected by treatment with 20% piperidine in DMF for 30 min and the wash steps were repeated. The Fmoc-Gly-OH was added in the presence of 2 equivalents of HOBT (hydroxybenzotriazole), 2 equivalents of HATU (2-(1H-7-azabenzotriazol-1-yl)-1,1,3,3-tetramethyl uronium hexafluorophosphate) and 4 equivalents of DIPEA. The subsequent amino acids in the order of Fmoc-Arg(Pbf)OH, Fmoc-Lys-Dde and Fmoc-Phe-OH were conjugated using the same deprotection and conjugation protocol. Each conjugation step was performed for 2 h. Allyl deprotection was performed using chloroform and N-methylmorpholine in the presence of palladium catalyst in a N_2 atmosphere for 4 hours followed by amino group deprotection using 20% piperidine in DMF. Cyclization was carried out overnight in the presence of PyBOP (benzotriazol-1-yl-oxytripyrrolidinophosphonium hexafluorophosphate), DIPEA and DMF. This step was repeated for an additional 6 h. Further, the 1-(4,4-Dimethyl-2,6-dioxocyclohexylidene) ethyl (Dde) group was specifically cleaved by using 2% hydrazine hydrate in DMF. For synthesis of the amphiphiles, the 8-amino-3,6 dioxaoctanoic acid (ADA) groups were conjugated to the lysine side chain using the same protocol as for the amino acids. Finally, stearic acid was conjugated in the presence of PyBOP (4 equivalents) and DIPEA (8 equivalents). The amphiphile was cleaved from the resin by treating with TFA:TIS: H_2O (95:2.5:2.5) for 3 hrs. After removal of TFA, the amphiphile was precipitated using ether:hexane (50:50) mixture. The amphiphile was then separated by centrifugation and freeze dried before further analysis. The synthesis of linear RGD amphiphile (C18-ADA5-RGD) was carried out using the same protocol as previously reported [18] (Specific Details are provided in Supplementary Materials). All amphiphiles synthesized were characterized for molecular weight and purity using Matrix Assisted Laser Desorption/Ionization- Time of Flight (MALDI-TOF) and reversed phase HPLC (RP-HPLC) respectively.

Determination of Critical Micelle Concentration (CMC) and Aggregation Number

The CMC and aggregation number of the amphiphiles were assessed by spectrofluorimetric method using pyrene as the hydrophobic fluorescent probe. CMC determination was performed as described in (18). For determination of aggregation number, 50 μL of 0.6 μM pyrene was added to 3 mL of 100 μM amphiphile stock solution [S]. Increasing volumes of fixed concentration of 1 mM cetylpyridinium chloride solution as quencher were added and fluorescence spectra were recorded at an excitation wavelength of 337 nm and emission wavelength of 373 nm. The fluorescence intensity in absence of quencher (I_0) and in presence of different concentrations of quencher (I) were determined and ln (I_0/I) was plotted against quencher concentration (Q). The slopes were determined from the linear relationship and aggregation number (N_{agg}) was calculated using following equation: ln (I_0/I) = Q* N_{agg}/([S]-CMC)

Determination of Size and Shape of RGD Micelles Using Transmission Electron Microscopy (TEM)

The peptide amphiphiles were dissolved completely in purified water at a concentration 10 times above CMC. A tiny dop (5 μL) of micelle solution was placed on the copper grid and the sample was air-dried. After air-drying, 5 μL of 2% *w*/*v* solution of phosphotungstic acid (pH 3.0) was placed on the sample. After 2 min, the excess stain was removed with a Whatman filter paper, and the sample on the grid was again air dried. The imaging of the sample was done using the Philips CM12 Transmission electron microscope operating at 100 kV and equipped with iTEM software.

Determination Paclitaxel Loading in the RGD Micelles

Paclitaxel was solubilized in the micelles at increasing concentrations above CMC of the amphiphile and analyzed using the same procedure as described in (18). Molar solubilization capacity (κ) of the amphiphiles is determined using the formula,

$$(\kappa) = (S_{total} - S_w) \Big/ C_{surfactant} - CMC$$

Determination of *In Vitro* Cargo Exchange of the Micelles on Dilution With Water Using Forster Resonance Energy Transfer (FRET)

The in vitro cargo exchange of the micelles was assessed by a FRET based method. Briefly, 2.5 mM solution of FRET dyes, DiI and DiO in DMF were mixed with amphiphiles present at a concentration 30 fold above CMC, and the final micelles were obtained after removal of the solvent by dialysis through a 1000 kDa membrane. The fluorescence spectra at an excitation wavelength of 484 nm and emission wavelength range of 495–600 nm were recorded after diluting the micelles 10 times with water or methanol. When micelle structure is intact (in water media), the FRET dyes are present in close proximity in the micelle core, and they therefore exhibit FRET transfer from donor (DiO) to receiver dye (DiI) and emission was at its maximum at 565 nm. On the other hand, the dilution of micelles in methanol, results into disruption of these micelles, which causes the FRET dyes to release into the medium resulting in no energy transfer. Therefore, DiO was monitored using the emission maximum which is observed at 510 nm. The FRET efficiency (also known as FRET ratio) was obtained from the ratio $I_{565}/(I_{565}+I_{501})$. To determine the cargo exchange, the micelles were prepared individually loaded with both the FRET dyes and mixed with water in the ratio 1:1:8, and the time resolved spectra were recorded for 24 h.

Determination of Competitive Binding of RGD Micelles to $\alpha_v\beta_3$ Integrin

The competitive binding assessment of the RGD amphiphiles (below CMC) and micelles (above CMC) was performed using fluorescence polarization (FP) assay adapted from the procedure reported by Wang *et al.* [21]. The FP assay was performed using a 384 well plate with total assay volume of 20 μL in each well [22]. A concentration of 300 nM of human $\alpha_v\beta_3$ integrin protein was selected from a saturation curve plotted using fixed concentration of 5 nM fluorescent probe, Cyclo[−RGDy-K(5-FAM)], and increasing concentrations of human $\alpha_v\beta_3$ integrin protein. The difference in the polarization values (in mP units) of the free probe and the protein-bound probe was used to determine the "dynamic range" for the assay. All amphiphiles including negative control, above and below CMC were dissolved in DMSO and further diluted in Tris buffer. Positive control cyclo (−RGDfK) was dissolved in Tris buffer. The final assay was performed by adding human $\alpha_v\beta_3$ integrin protein (final concentration of 300 nM), fluorescent probe Cyclo[−RGDy-K(5-FAM)] (final concentration of 5 nM) and the test amphiphiles (final concentration of 4 μM and 10 times above CMC) in the same order into the individual wells. The fluorescence polarization values were measured at an excitation wavelength of 485 nm and emission wavelength of 525 nm using a SpectraMax M5 Microplate Reader (Molecular Devices, CA, USA) immediately upon mixing and after 15 min incubation. The percentage of probe displaced by the test compound was calculated using the following formula:

$$\%\ Probe\ displaced = 100 - \left(\frac{[mP\ of\ test\ well - mP\ of\ probe\ only\ well]}{dynamic\ range} \times 100 \right)$$

Cellular Internalization of RGD Micelles

FITC-loaded RGD micelles in serum free media at a concentration 10 fold higher than CMC were prepared by using the same method as that of paclitaxel-loaded RGD micelles and the final concentration of FITC in the aqueous medium was 200 μg/mL. A2058 melanoma cells were cultured in T75 flasks incubated at 37°C and 5% CO_2. Upon reaching 80–90% confluency, the cells were counted and seeded on the coverslips placed inside 6-well plates at a density of 3,50,000 cells/well. The cells were allowed to attach for 24 h before the experiment was performed. Upon attachment, the cells were washed twice with HBSS and serum free media and then treated with FITC-loaded C18-ADA5-RGD, C18-ADA5-cRGDfK, C18-ADA5-GGG micelles, and equivalent concentration of free FITC for different predetermined time intervals at 37°C, following which the medium was removed, and the cells were washed twice with HBSS. The cells were treated with a 5 μM solution of Alexa fluor 594 wheat germ agglutinin in HBSS for 10 min to stain the plasma membrane. After washing and fixing the cells using 4% paraformaldehyde solution, coverslips were mounted on microscopic slides using mounting medium (slow fade gold) and images were taken on a Leica DMIRE2 confocal laser scanning microscope using 64× magnification and oil immersion in the FITC channel (491 nm) and Texas Red channel (561 nm). For determining the mechanism of cellular uptake, the same experiment was performed at 4°C to study the effect of temperature on cellular uptake. Additionally the mechanism of cellular uptake was studied by pretreating the cells with 0.45 M sucrose for 20 min followed by treatment with micelles. Using 12 random cells in each sample, the relative fluorescence inside the cells was quantified using the Metamorph software.

Cytotoxicity Analysis of RGD Micelles

The cytotoxicity study of free paclitaxel and paclitaxel-loaded micelles in A2058 melanoma cells and Detroit 551 keratinocyte cells was performed in the concentration range of 0.1 to 200 nM using the SRB colorimetric assay using the procedure described in (18). The percentage viability of cells was plotted as a function of log paclitaxel concentration ($n=4$) and data were analyzed in Graph Pad Prism, Version 5.0 d software (GraphPad Software Inc, CA, USA) using nonlinear-regression curve fit.

In Vivo Assessment in Mice Melanoma Xenograft Model

The *in vivo* study was performed as per the animal protocol (No.13R04a) reviewed and approved by Institutional Animal Care and Use Committee (IACUC). Four to five week old female athymic nude mice (homozygous) (nu/nu) were kept in sterilized cages and provided with sterilized rodent diet and water. The A2058 cells (10,00,000 cells/mouse) were injected subcutaneously using a 26-gauge needle on the right or left posterior flank or on the back of mice. When visible tumors (2–4 mm) were observed, mice were divided into 3 treatment groups (control group, paclitaxel in Cremophor EL-treated group, and paclitaxel-loaded RGD micelle-treated group); each group consisted of six mice. The day dosing started was considered as day zero and a dose of 50 μg of paclitaxel per kg of body weight was injected twice weekly via tail vein. In the second study, the dosing frequency was increased to every alternate day. The body weight of mice was noted and tumor size (in mm) was measured using vernier caliper three times every week. The tumor volume was calculated using the formula as follows:

$$Tumor\ volume\ \left(mm^3\right) = \frac{(D) \times (d)^2}{2}$$

Where "D" is the long axis and "d" is the short axis of the tumor lump. The tumor size reaching 20×20 mm marked end of the treatment period and mice were euthanized using CO_2 at this time. The plot of tumor volume vs. days was statistically evaluated using GraphPad Prism software.

Statistical Analysis

The experimental results are presented as Mean ± *SD* or Mean ± *SE* as stated. To determine statistical significance, *t*-test was performed at a p value of 0.05. For *in vivo* experimental data, unpaired *t*-test performed at p value of 0.05 was used to compare the control group with each treatment group. To compare all the three treatment groups, a two way-ANOVA was performed at a p value of 0.05 along with Bonferroni post hoc test.

RESULTS

Design and Synthesis of RGD Peptide Amphiphiles

We designed, synthesized and purified the RGD peptide amphiphiles containing linear and cyclic RGD ligands (Fig. 1). The molecular modeling studies performed using Molecular Operating Environment software showed that the cyclic RGD peptide (cRGDfK) exhibited lower binding energy and greater number of binding interactions with the $\alpha_v\beta_3$ integrin in comparison with the linear RGD peptide (RGD). The cyclic RGD showed a binding score of −21.8 kcal/mol and a total of 21 binding interactions whereas, the linear RGD ligand only exhibited 15 total binding interactions and a high binding score of −5.8 kcal/mol, indicating that the cyclic RGD was a better ligand for integrin binding. Previously published data have indicated that cyclic RGD exhibits lower IC_{50} value

(a) C18-ADA5-RGD

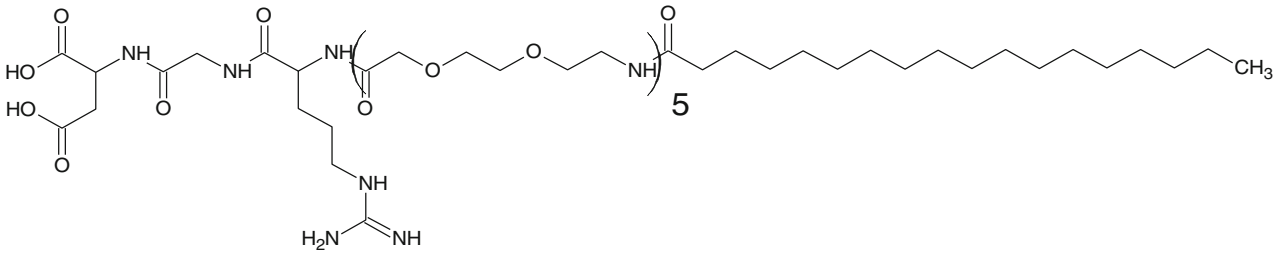

(b) C18-ADA5-cRGDfK

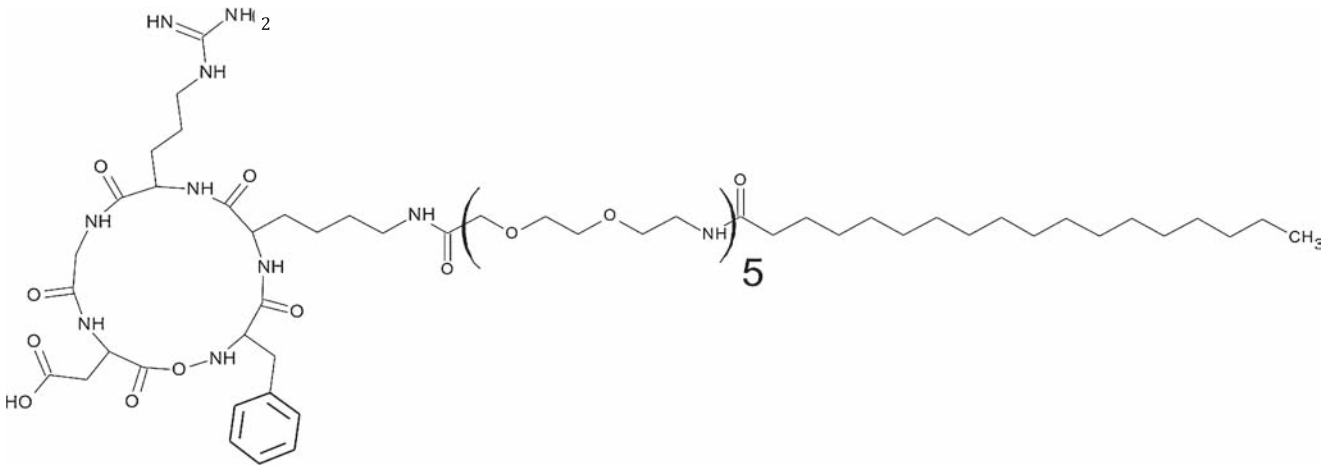

(c) C18-ADA5-GGG

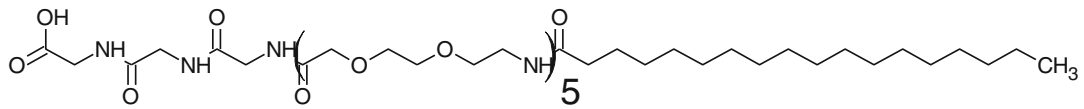

Fig. 1 Molecular Structure of the different linear RGD, cyclic RGD and control amphiphile.

compared with that of its linear counterpart, this is probably due to the improved conformational stability as observed in the modeling studies [23]. However, the affinity of the ligand is not the only factor that determines the interaction between the protein and the ligand in a self-assembly. The utility of the amphiphiles as successful targeted drug delivery vehicles is affected by many other factors apart from the ligand binding affinity for the integrin receptor. Therefore, in order to select a better drug delivery vehicle, both cyclic and linear RGD amphiphiles were synthesized and tested for the hypothesis. The synthesized peptide amphiphiles were separated using HPLC with a purity of more than 90% and characterized for molecular weight. The molecular ion peak at m/z of 1338.9 and 1595.9 confirmed the formation of C18-ADA5-RGD and C18-ADA5-cRGDfK amphiphiles respectively, whereas, the negative control C18-ADA5-GGG amphiphile was confirmed from the sodium adduct peak at m/z of 1203 (Details in Supplementary material).

Determination of Critical Micelle Concentration (CMC) and Aggregation Number

We performed further characterization studies concerning the self-assembly of these amphiphiles (see supplementary material for details). We used pyrene as the hydrophobic fluorescent probe to determine the CMC and aggregation number by fluorescence spectroscopy. The changes in the solvent environment of pyrene upon its incorporation into the

hydrophobic core of the micelle were detected from changes in the excimer and monomer peak ratio in the fluorescence spectra. The CMC values (see supplementary material for details) of each of the amphiphiles are shown in Table I. The CMC values of the amphiphiles recorded were in lower micromolar concentration range and are comparable to the CMC of most polymeric surfactant micelles that are in the range of 10^{-4} to 10^{-5} M and is much lower compared with the CMC of the conventional non-ionic amphiphiles that are in the range of 10^{-3} to 10^{-4} M [24]. Our previously synthesized amphiphiles, C16-ADA2-RGD and C18-ADA2-RGD produced CMC's of 30 μM and 9 μM respectively. Longer hydrophilic linker increased the CMC of the C18-ADA5-RGD amphiphile, and the amphiphile is soluble upto 100 fold their CMC concentration whereas the C18-ADA2-RGD amphiphiles were soluble only upto 10 fold above their CMC. The cyclic RGD amphiphile had a comparable CMC to the previously studied C18-ADA2-RGD amphiphiles. The micelle concentration was determined by "steady state fluorescence quenching" using pyrene as the fluorescent probe and cetylpyridinium chloride as the quencher [25]. The aggregation number, which is the number of amphiphiles present in each micelle, was determined indirectly from the micelle concentration. The micelles had aggregation number in the range of 12–16.

Table I CMC and Aggregation Number of the Peptide-Based Amphiphiles

Amphiphile	CMC (μM)	Aggregation number
C18-ADA5-RGD	25.7 ± 5.8	12
C18-ADA5-cRGDfK	8.0 ± 1.0	15
C18-ADA5-GGG	23.3 ± 2.8	16

Determination of Size and Shape of RGD Micelles Using Transmission Electron Microscopy (TEM)

The size and morphology of the micelles determined from the transmission electron microscopy using negative staining is shown in Fig. 2. The amphiphiles formed spherical aggregates with particle sizes in the range of 10–25 nm. Compared with the simple fatty acid-RGD conjugates and our other previously developed linear RGD amphiphiles, which formed larger aggregates [19, 22], the particle sizes were greatly reduced upon addition of multiple units of the hydrophilic ADA linker. The addition of long ADA chains, which are known to be flexible linkers, made the interface less rigid, possibly resulting in greater curvature between the head and tail region of the amphiphiles. The increase in the curvature of the micelle interface may have resulted into lower particle sizes as seen from the trend in the data which is also consistent with reported trends [26].

Determination Paclitaxel Loading in the RGD Micelles

In addition, ADA linkers played a significant role in improving the solubility of the amphiphiles in water, so that micelle solutions at much higher concentrations above CMC were able to dissolve the drug effectively. Paclitaxel solubility in C18-ADA5-RGD and C18-ADA5-cRGDfK micelles increased linearly with amphiphile concentration ($R^2 > 0.98$) (Fig. 3) and the molar solubilization capacity (κ) determined from the plot of total solubility of paclitaxel against the total concentration of amphiphile was found to be 0.0103 and 0.007, respectively. Compared with the aqueous solubility of paclitaxel (0.4 μg/mL), the micelles increased the solubility of the drug by 35 fold at the tested amphiphile concentrations. Considering that the amphiphiles could be solubilized in water upto 100 fold above their CMC, the solubilization capacity of the amphiphiles improved compared to those we previously developed [18, 19, 22].

Determination of in Vitro Cargo Exchange of the Micelles on Dilution With Water Using FRET (Forster Resonance Energy Transfer)

The entrapment efficiency of the hydrophobic FRET dyes in the core of the micelle was 0.9 and 0.94 for the C18-ADA5-RGD and C18-ADA5-cRGDfK micelles diluted in water at a concentration 3 fold above their CMC. The dilution in methanol at concentrations 3 fold above CMC disrupted the core of the micelle by dissolving the amphiphile and the dye and this resulted in the loss of FRET (Fig. 4). The ability of the micelles to retain the entrapped cargo in its core without releasing them prematurely is very important for the success of targeted drug delivery. This property was assessed by evaluating the extent of partitioning or exchange of cargo between micelle populations [27]. Upon loading the FRET dyes in separate micelle populations, FRET was not observed at initial time points. For C18-ADA5-RGD micelles, low FRET efficiency was maintained for 24 h, however for C18-ADA5-cRGDfk micelles, FRET efficiency increased by 115% in 24 h indicating that the micelles showed rapid exchange of entrapped dyes, which would influence its efficacy as a drug delivery system (Fig. 5). Overall, the FRET study provided some insight into the stability of the RGD micelles and can help in the selection of amphiphiles for drug delivery applications.

Determination of Competitive Binding of RGD Micelles to $\alpha_v\beta_3$ Integrin

The ability of the micelles to bind to the target protein and to internalize into the integrin over-expressing cells was assessed by in vitro assays. Competitive binding determines the ability

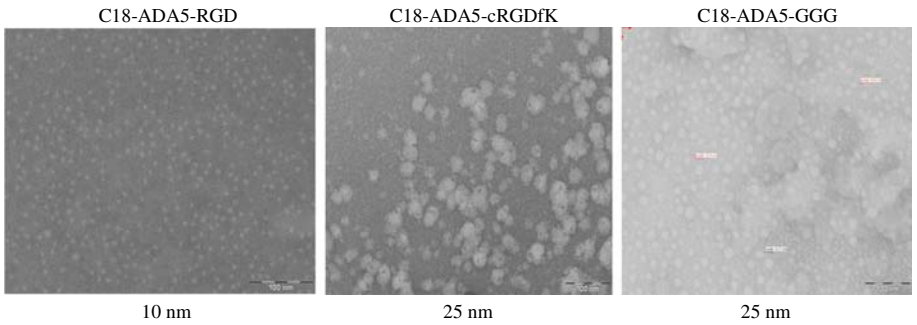

Fig. 2 TEM micrographs and average sizes of the different RGD micelles (*Scale bar*:100 nm).

of a compound to displace a ligand already bound to the protein. The cyclic RGD ligand used as a positive control exhibited more than 90% displacement of the integrin bound fluorescent probe and this proved the effectiveness and reliability of the competitive FP assay. All the RGD amphiphiles were assessed for competitive binding to the $\alpha_v\beta_3$ integrin receptors below and above their CMCs. We observed that the cyclic RGD amphiphile below CMC could displace as much as 72% of the bound cyclic RGD probe. The cyclic RGD amphiphiles above CMC also exhibited decent binding, displacing 53% of the bound probe (Fig. 6). The linear RGD amphiphiles were able to displace 43 and 52% of the bound probe at concentrations above and below CMC, respectively. No change in the polarization values was observed after incubation for 15 minutes indicating that the binding was a fast order kinetic process. The C18-ADA5-GGG amphiphiles showed less than 15% displacement of bound probe at both the tested concentrations thereby confirming the $\alpha_v\beta_3$ integrin binding specificity of the RGD peptide amphiphiles. The cyclic RGD amphiphiles had higher binding than the linear RGD amphiphiles synthesized (C18-ADA-RGD, C18-ADA2-RGD and C18-ADA5-RGD) [22].

Cellular Internalization of RGD Micelles

The uptake of RGD micelles into integrin overexpressing A2058 melanoma cells was studied with the aid of confocal microscopy by following the internalization of fluorescent dye

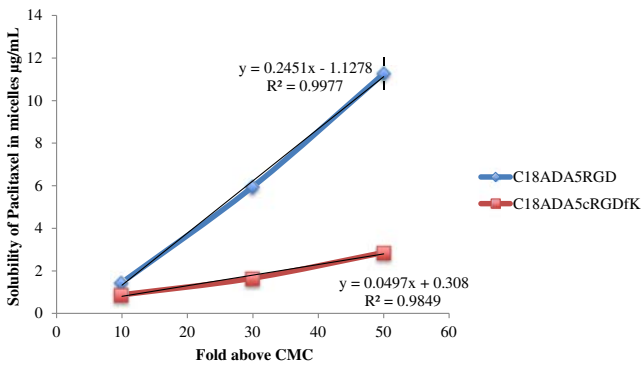

Fig. 3 Paclitaxel solubility in different RGD micelles at increasing concentration above CMC.

FITC, physically entrapped in micelles Fig. 7. The FITC-loaded C18-ADA5-cRGDfK micelles internalized within the first few minutes of incubation at 37°C (Fig. 7). In contrast, the FITC-loaded C18-ADA5-RGD micelles exhibited only surface binding at the initial time points. After 20 min of incubation, significant internalization of the dye was observed in the cells incubated with micelles compared with the cells incubated with FITC only. The FITC-loaded C18-ADA5-GGG control micelles showed no significant internalization in 20 min thus confirming the integrin receptor-mediated cell uptake specificity of the RGD micelles. The internalization of the

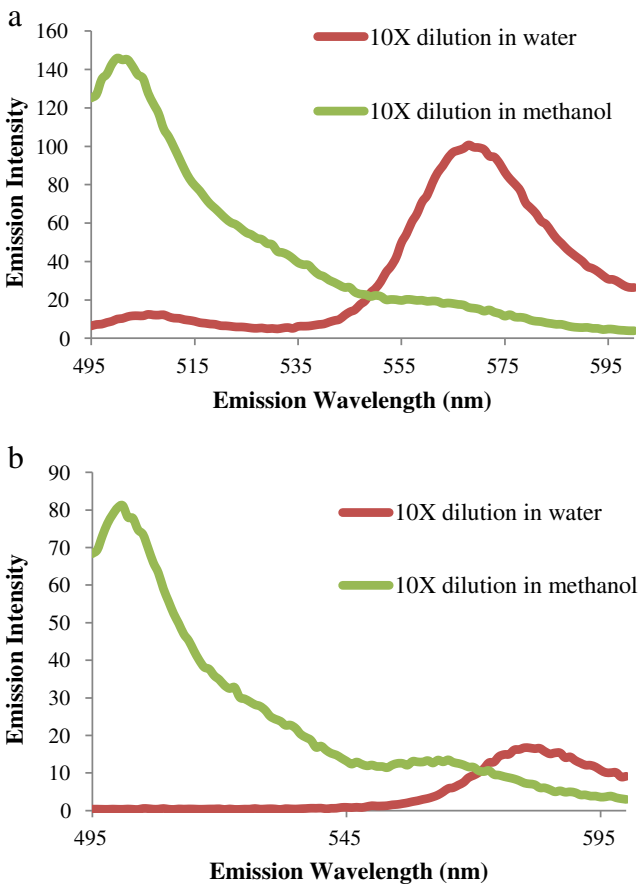

Fig. 4 Emission spectra of DiI + DiO loaded in (**a**) C18-ADA5-RGD micelles and (**b**) C18-ADA5-cRGDfK micelles diluted 10 fold in water and 10 fold in methanol. The concentration of amphiphiles on 10-fold dilution is 3 times above CMC.

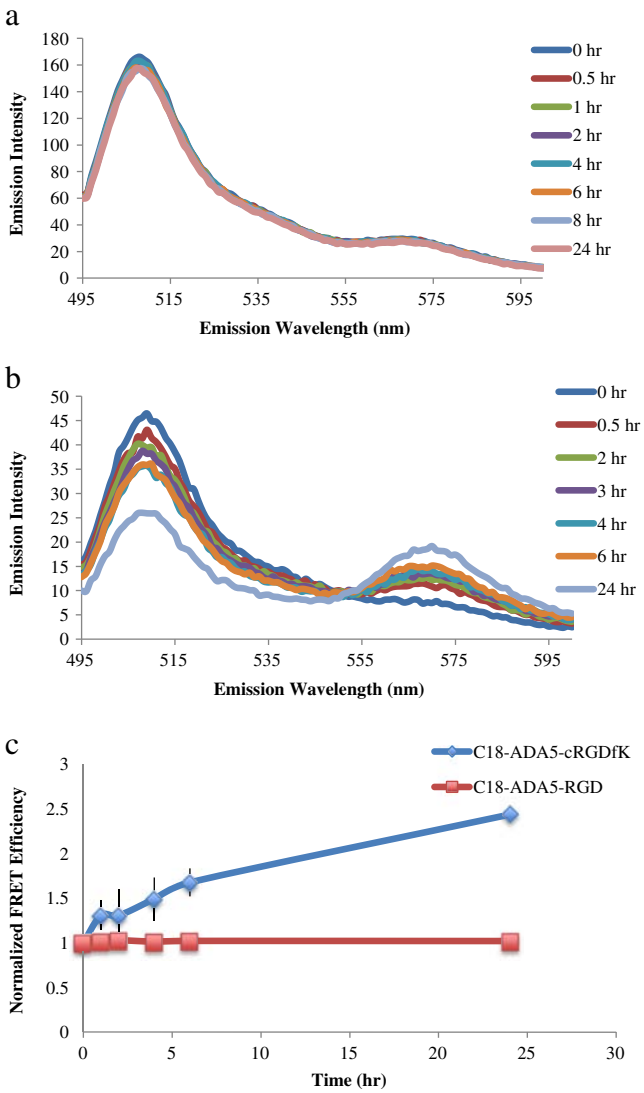

Fig. 5 Time resolved emission spectra of (**a**) separate DiO loaded C18-ADA5-RGD micelles and DiI loaded C18-ADA5-RGD micelles (**b**) separate DiO loaded C18-ADA5-cRGDfK micelles and DiI loaded C18-ADA5-cRGDfK micelles, mixed and diluted up to 10 fold in water (**c**) Change in normalized FRET efficiency upon mixing the DiO loaded micelle and DiI loaded micelle populations over 24 h (Mean ± SD).

RGD micelles into the melanoma cells was observed at metabolically viable temperature of 37°C, whereas the uptake was inhibited at 4°C; therefore receptor-mediated endocytosis should be the proposed mechanism of the cellular uptake (Fig. 7). [28–30]. Further confirmation of the proposed mechanism of endocytosis was obtained by pre-treating the cells with an endocytosis inhibitor prior to incubating the cells with the micelles. Hypertonic sucrose solution (0.45 M) is known to disrupt clathrin coated pits associated with the receptor-mediated endocytosis process. The hypertonic sucrose treatment significantly inhibited the uptake of the FITC-loaded RGD micelles as indicated by the reduced fluorescence emission inside the cells. The quantification of fluorescence intensities corresponding to cellular uptakes showed that compared with free FITC, the FITC-loaded linear and cyclic RGD amphiphiles displayed 2 and 5 fold higher cell internalization capacity, respectively (Fig. 8). Overall the studies proved that the $\alpha_v\beta_3$ integrin over expressing cells enhanced the internalization of RGD micelles in comparison with control micelles and free cargo.

Cytotoxicity Analysis of RGD Micelles

The cytotoxicity of paclitaxel loaded in RGD micelles and as free drug was assessed in melanoma cells to identify targeting specificity. Data from cytotoxicity studies were obtained after a treatment period of 72 h since cytotoxic efficacy of paclitaxel was reported to be maximum when cells were exposed to the drug for a prolonged period [31]. Upon treatment with blank micelles, the presence of high number of viable cells indicated that the blank micelle controls were non-toxic to the cells. The hypothesis is that if the drug-loaded carriers are internalized via an active uptake process, then the extracellular concentration of the drug required to achieve an equivalent cytotoxic effect will be much lower than that of the free drug. This hypothesis was confirmed by comparing the IC_{50} values of paclitaxel with the experimental IC_{50} values obtained with micelle treatment. For example, treatment with free paclitaxel exhibited an IC_{50} of 7.6nM whereas treatments with paclitaxel loaded in C18-ADA5-RGD and C18-ADA5-cRGDfK micelles exhibited an IC_{50} of 2.5 and 2.1 nM, respectively (Fig. 9). In normal Detroit 551 keratinocyte cells, the IC_{50} of free paclitaxel was found to be 4.7 nM whereas the IC_{50} for paclitaxel-loaded C18-ADA5-RGD and C18-ADA5-cRGDfK micelles was found to be 33.8 and 13.5 nM, respectively (Fig. 9). On the whole, the cytotoxicity trends were comparable with that of other targeted nanoparticulate systems [32].

In Vivo Assessment in Mice Melanoma Xenograft Model

The results of cytotoxicity were further confirmed by *in vivo* testing of the paclitaxel-loaded RGD micelles. The homozygous athymic nude mice used in the study are genetically modified mice which lack a thymus and therefore are T-cell deficient. This causes significant loss of activity against thymus dependent antigens and the mice cannot reject the injected tumor cells or xenografts. The A2058 cells produced visible solid tumors in the immune compromised mice in 2 weeks of innoculation. The paclitaxel-loaded C18-ADA5-RGD micelles were selected for further testing in the animal model since the C18-ADA5-cRGDfK micelles did not show sufficient enhancement in paclitaxel solubility to deliver an appreciable dose of the drug. Considering the highest solubility of paclitaxel in the micelles at 50X CMC, a dose of 50 μg/kg could be administered at one time. A therapeutic dose of paclitaxel could not be administered to the mice since the

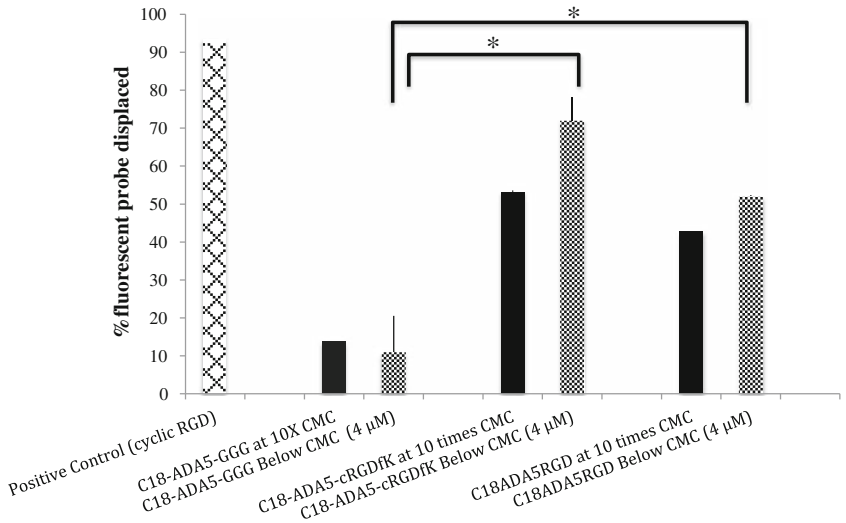

Fig. 6 Competitive binding of different RGD amphiphiles to human $\alpha_v\beta_3$ integrin protein above and below CMC concentrations (Mean ± SE) *Statistically significant at $P \leq 0.05$.

micelles did not have enough solubilization capacity to administer higher doses of paclitaxel. Therefore, instead of tumor regression, the difference in tumor growth progression was studied by administering a sub-therapeutic dose of paclitaxel in the RGD micelles. In order to confirm the effect of the sub therapeutic dose on the tumor progression, 2 separate studies were conducted with increased dosing. The dose of paclitaxel (50 μg/kg twice weekly) was elevated by increasing the frequency of dosing (50 μg every alternate day). The administered dose did not produce tumor regression, however a noticeable difference in the tumor growth was observed between the control and the treatment groups. The differences in tumor growth had been previously used to assess the efficacy of drugs and different treatment methods [12]. For both twice weekly and alternate day dosing regimens, the tumor growth in the control group was higher than the tumor growth in the treatment groups; the treatment groups also showed much lower tumor volumes (Figs. 10 and 11). Treatment with paclitaxel-loaded RGD micelles produced a significant difference in tumor volumes when compared with control ($p < 0.05$) whereas, inhibition of tumor growth produced by the non-targeted micelles was found to be statistically insignificant. For the twice weekly dosing regimen, after the completion of treatment period, tumor inhibition compared with respective controls was only 28.2% for standard paclitaxel formulation in Cremophor EL and as much as 61.8% for paclitaxel-loaded RGD micelles. For alternate day dosing regimen, after the completion of treatment, tumor inhibition compared with respective controls was only 51.4% for standard paclitaxel in Cremophor EL and as much as 68.9% for paclitaxel-loaded RGD micelles. No significant loss in body weight was observed during RGD micelle treatment (Fig. 12). Treatment with paclitaxel in Cremophor EL was associated with a loss in body weight attributed to the toxic side-effects of Cremophor EL medium [33]. Overall, the findings from this study showed that paclitaxel loaded in RGD micelle was more effective compared with standard paclitaxel formulation in Cremophor EL in delivering the drug to the tumor cells. Therefore, this formulation has the potential for active targeting and site-specific delivery of paclitaxel in cancer cells.

DISCUSSION

Our group presented previously the concept of peptide amphiphiles of linear RGD as carrier for drug targeting. In this study, the linear and cyclic RGD peptide amphiphiles were compared for their potential as drug delivery carriers. Although cyclic RGD is a better targeting ligand than its linear counterpart, the drug delivery efficacy of the amphiphiles is determined by several factors such as self assembly and physicochemical characteristics of the micelles, kinetic stability of the micelles, extent of drug loading and interaction of multivalent system with the target protein alpha v beta 3 integrin. The study was performed to determine a better drug delivery carrier and evaluate the in vitro as well as *in vivo* targeting efficacy of the micelles. The complete on-resin synthesis of peptide amphiphiles was performed and the amphiphiles were characterized for the identity, purity and self assembly. The observed low CMC of the amphiphiles, in the micro molar range, indicated that the micelle solutions could withstand high extent of dilution in the body and which improves their chances of becoming promising drug delivery vehicles. The low molecular weight RGD amphiphiles had smaller aggregation numbers compared to conventional non ionic amphiphiles like polysorbates (Tweens). The relationship between amphiphile aggregation and micellization is described as:

$$N_{agg} = \frac{[S]-[CMC]}{[M]}$$

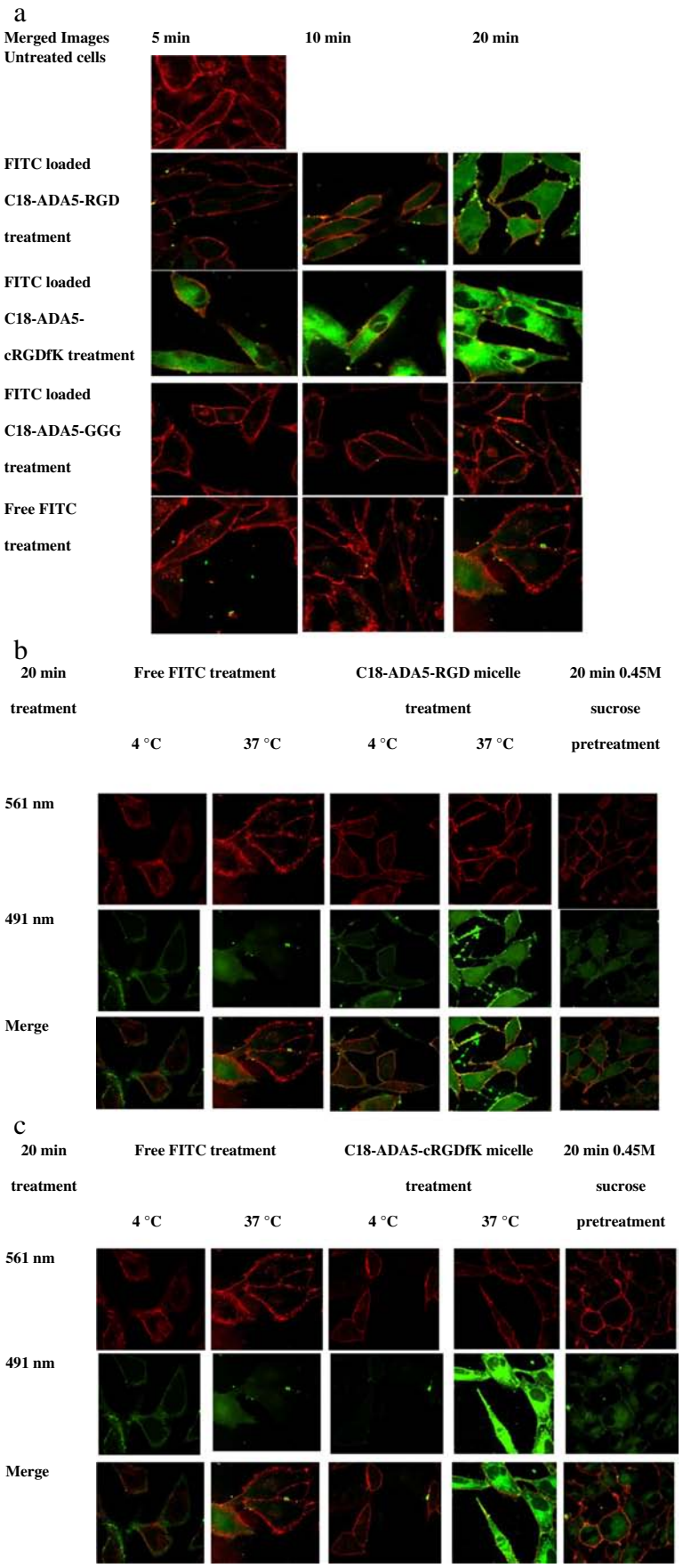

Fig. 7 (**a**) Confocal Images showing internalization of FITC loaded micelles and control treatments at different treatment times (**b**) Comparison of internalization of FITC loaded C18-ADA5-RGD micelles at different temperatures and in presence of endocytosis inhibitor (**c**) Comparison of internalization of FITC loaded C18-ADA5-cRGDfK micelles at different temperatures and in presence of endocytosis inhibitor (*Scale bar* 20 μm)

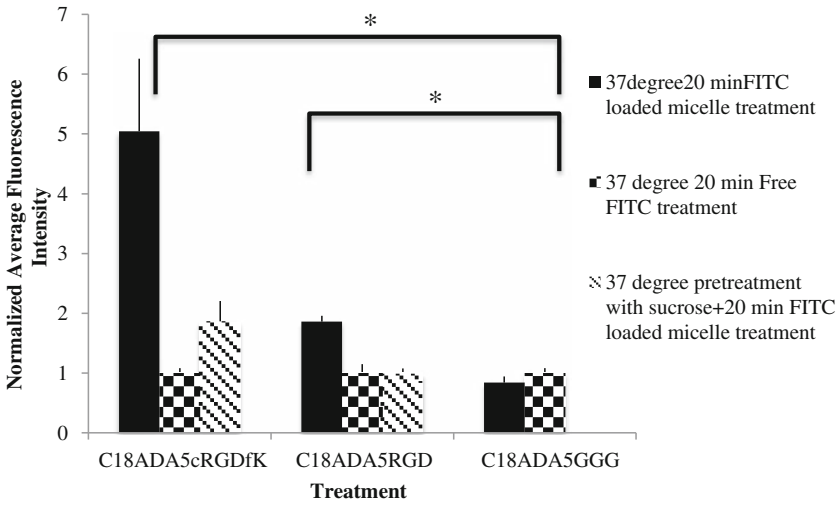

Fig. 8 Relative quantitative internalization of different FITC loaded RGD micelles and free FITC in A2058 melanoma cells under different conditions (Mean ± SD) (*Significant difference ($P < 0.0001$) between 37°C FITC loaded targeted micelle treatment and free FITC treatment as well as between 37°C FITC loaded targeted micelle treatment and micelle treatment in presence of 0.45 M sucrose).

where, [S] = Total concentration of amphiphile in solution, [M] = Total concentration of micelles in solution, CMC = Critical Micellar Concentration, N_{agg} = Aggregation Number of the micelle.

The aggregation number is dependent on factors such as length of hydrophobic chain, the size of the hydrophilic head group, addition of counter ions (for ionic surfactants) and so on. The trend in aggregation number corresponded well with the trends in micelle size. Although the addition of longer ADA linkers increased the CMC of the amphihiles, it also resulted into improvement in the solubility of the amphiphiles in water from 10 fold above CMC to 100 fold above CMC. The RGD micelles are proposed to follow the principles of enhanced permeation and retention (EPR) as well as ligand-protein interaction. The addition of the longer flexible ADA linker chain helped in reducing the micelle size thereby enabling potentially better targeting by EPR followed by molecular interaction between ligand and target protein as well as

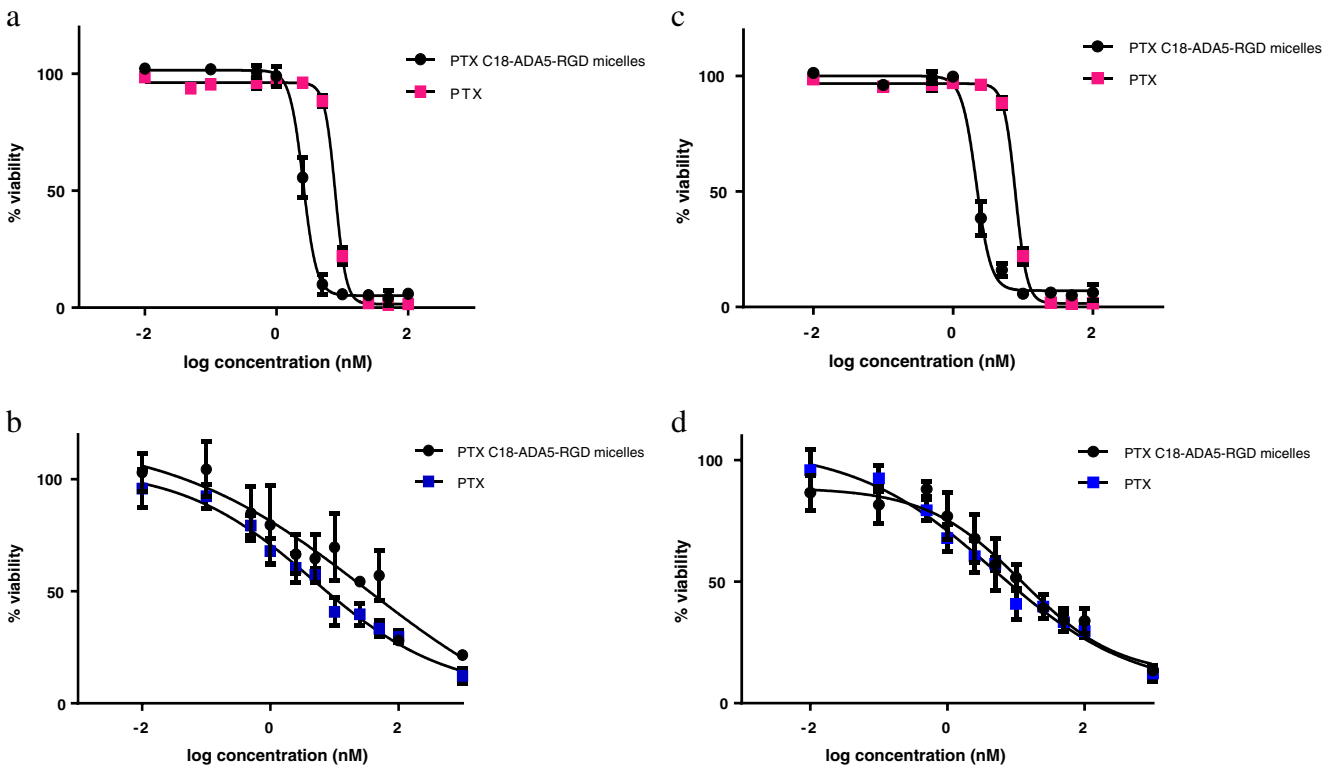

Fig. 9 Comparison of cytotoxicity of (**a**) free paclitaxel (PTX) and paclitaxel loaded in C18-ADA5-RGD micelles in A2058 cells (**b**) free paclitaxel (PTX) and paclitaxel loaded in C18-ADA5-RGD micelles in Detroit 551 cells (**c**) free paclitaxel (PTX) and paclitaxel loaded in C18-ADA5-cRGDfK micelles in A2058 cells (**d**) free paclitaxel (PTX) and paclitaxel loaded in C18-ADA5-cRGDfK micelles in Detroit 551cells (Mean ± SD).

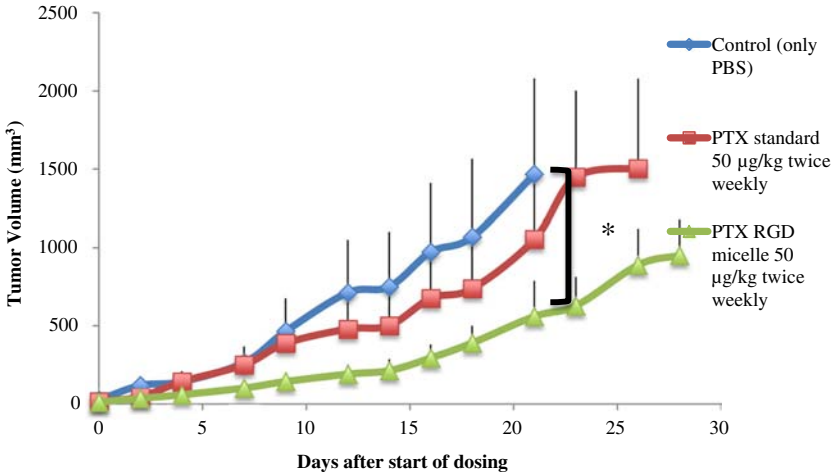

Fig. 10 Tumor growth curves obtained when mice with A2058 xenograft are treated with 50 μg/kg of paclitaxel twice weekly in standard Cremophor micelles (Taxol) and in C18-ADA5-RGD micelles (Mean ± SE). Control treatment includes only PBS. * Significant difference ($p \leq 0.05$) with unpaired two-tailed *t*-test observed between control and PTX RGD micelle 50 μg/kg twice weekly treatment. Overall comparison of all three groups in ANOVA showed no significant difference in treatments at $p \leq 0.05$.

better penetration into tumor tissues [4]. The drug paclitaxel was an ideal model drug for loading into the micelle system due to its high hydrophobicity and extremely poor aqueous solubility. As the concentration of amphiphiles was increased the paclitaxel solubility was enhanced, with about 35-fold increase in paclitaxel solubility observed at a concentration of 50 fold over CMC of the linear RGD amphiphiles. However, the solubility enhancement was limited by the concentration of amphiphiles that could be administered for safe delivery. In agreement with previously reported trends, the cyclic RGD amphiphile showed higher binding to pure alpha v beta 3 integrin protein compared to the linear RGD amphiphile as observed in the fluorescence polarization studies [23]. However both the cyclic RGD amphiphiles as well as linear RGD amphiphiles had higher binding potential as individual ligand (below CMC concentrations) compared to the binding of multivalent assembly or micellar form (above CMC concentrations). It has been previously suggested that integrin receptor is present in clusters on cell surface and therefore multivalent ligands may show enhanced binding to the integrin receptor [10]. Interestingly, results of this study indicated that multivalent system might actually reduce binding interaction possibly due to increase in steric bulk resulting from the formation the micelles. Although the cyclic RGD amphiphiles had better receptor binding and affinity compared to the linear RGD amphiphiles, the objective was to compare the overall drug delivery efficacy of these micellar carriers and this was achieved by evaluating different drug delivery parameters

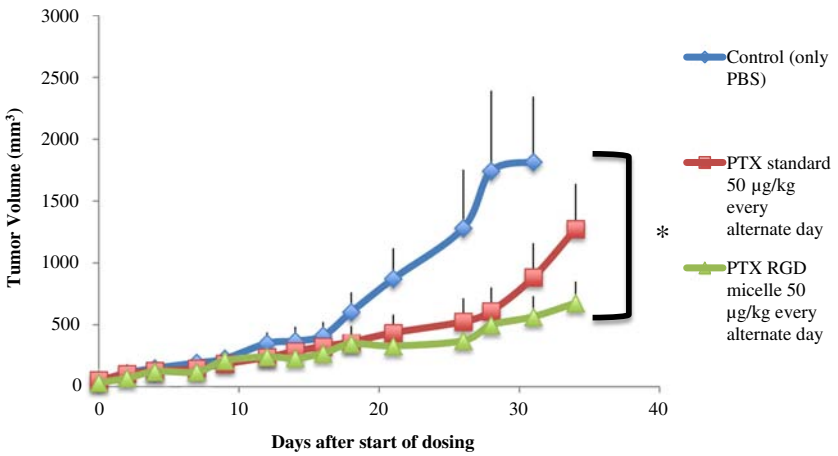

Fig. 11 Tumor growth curves obtained when mice with A2058 xenograft are treated with 50 μg/kg of paclitaxel every alternate day in standard Cremophor micelles (Taxol) and in C18-ADA5-RGD micelles (Mean ± SE). Control treatment includes only PBS. * Significant difference ($p \leq 0.05$) with unpaired two-tailed *t*-test observed between control and PTX RGD micelle 50 μg/kg every alternate day treatment. Overall comparison of all three groups in ANOVA with Bonferroni post hoc test showed significant difference between means of Control v/s PTX standard Cremophor micelles 50 μg/kg every alternate day treatment at Day 28, 31 and Control v/s PTX RGD micelle 50 μg/kg every alternate day treatment at Day 26, 28 and 31.

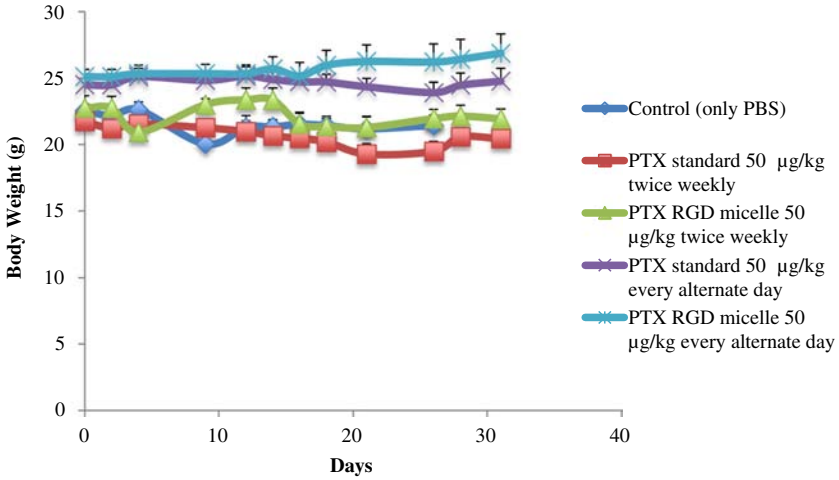

Fig. 12 Body weight of mice in different groups throughout the period of treatment.

including the stability of the micelles and the drug loading. FRET studies revealed the relative stability of the linear and cyclic RGD amphiphile micelles on dilution. The self-assemblies formed by cyclic RGD micelles were not found to be stable over time and showed significant exchange of entrapped FRET dyes, which could potentially affect their utility as effective carriers. On the other hand the linear RGD micelles showed no exchange of entrapped FRET dyes between micelle populations and formed strong assemblies which was a desirable feature for delivering drugs to tumor site. The mechanism of cellular internalization of the micelles physically entrapped with a fluorescent dye FITC was confirmed to be via an endocytosis process. Since both passive diffusion and active cellular uptake are energy dependent processes, the mechanism was studied using temperature dependent studies as well as by treatment with endocytosis inhibitor. The FITC loaded C18-ADA5-cRGDfK micelles showed higher internalization compared to FITC loaded linear C18-ADA5-RGD micelles, which was in agreement with the results from the binding study. The results of cytotoxicity studies proved the targeting efficacy of RGD micelles for delivering paclitaxel, as observed from the fact that much lower extracellular concentrations of the drug were required for achieving cytotoxicity when delivered in the form of micelles. The paclitaxel delivered in cyclic RGD micelles exhibited the slightly lower IC50, which showed that it had better targeting efficacy. The difference in IC50 of paclitaxel between the integrin over expressing cells and normal cells was an indicator of the specificity of the vehicle. The lower specificity for paclitaxel-loaded C18-ADA5-cRGDfK micelles could be attributed to the lower kinetic stability of these micelles as observed in the FRET studies, resulting in the premature release of the entrapped paclitaxel. Although cyclic RGD micelles had comparatively better targeting and internalization efficacy, owing to the higher drug solubilization capacity, better stability and greater specificity, the C18-ADA5-RGD micelles were a better drug delivery vehicle and were tested *in vivo* in tumor xenograft mice model. The *in vivo* studies proved that paclitaxel delivered in RGD micelles was more effective in inhibiting tumor growth compared to the paclitaxel delivered in cremophor vehicle. However, higher doses of paclitaxel, capable of producing tumor regression could not be administered due to their relatively lower solubilization capacity for the drug in the RGD micelles compared to conventional non-ionic surfactant micelles and the limitation on amount of amphiphiles that could be administered to avoid any safety concerns. Other formulation strategies like mixed micelle approach and further optimization of amphiphile design will be useful to overcome these limitations in the future studies.

CONCLUSION

The findings from this study showed that RGD based amphiphiles could form nano-sized spherical micelles through self-assembly. The RGD micelles could bind specifically to the $\alpha_v\beta_3$ integrin proteins and had undergone cellular internalization in melanoma cell lines overexpressing $\alpha_v\beta_3$ integrin receptors via receptor-mediated endocytosis. The enhanced cytotoxicity of the paclitaxel-loaded RGD micelles was confirmed from both in vitro and *in vivo* studies. Although the cyclic RGD amphiphiles showed higher binding, increased cellular uptake, and cytotoxicity, its utility as a drug carrier was limited by poor solubility and high cargo exchange. Overall, results from our study proved that self-assembly of peptide amphiphiles can be a promising strategy for active targeting and site-specific delivery of hydrophobic drugs. In future, effective structural modifications (introduction of crosslinking in the peptide chain) or optimization of formulation strategies (formation of mixed micelles) can be used to fine-tune drug loading and drug retention capacity of these potential carriers for application in targeted drug delivery.

ACKNOWLEDGMENTS AND DISCLOSURES

Authors would like to thank Dr. Mamoun Alhamadsheh (Department of Pharmaceutics and Medicinal Chemistry) for his inputs on fluorescence polarization assay.

REFERENCES

1. de Boer-Dennert M, de Wit R, Schmitz PI, Djontono J, v Beurden V, Stoter G, *et al.* Patient perceptions of the side-effects of chemotherapy: the influence of 5HT3 antagonists. Br J Cancer. 1997;76(8):1055–61.
2. Torchilin V. Drug targeting. Eur J Pharm Sci. 2000;11(2):S81–91.
3. Gelderblom H, Verweij J, Nooter K, Sparreboom A. Cremophor EL: the drawbacks and advantages of vehicle selection for drug formulation. Eur J Cancer. 2001;37(13):1590–8.
4. Dong H, Dube N, Shu J, Seo J, Mahakian L, Ferrara K, *et al.* Long circulating 15 nm micelles based on amphiphilic 3-helix peptide-PEG conjugates. ACS Nano. 2012;6(6):5320–9.
5. Mizejewski J. Role of integrins in cancer: survey of expression patterns. Proc Soc Exp Bio Med. 1999;222(2):124–38.
6. Xiong J, Stehle T, Zhang R, Frech M, Goodman SL, Arnaout MA. Crystal structure of the extracellular segment of integrin $\alpha_v\beta_3$ in complex with an Arg-Gly-Asp ligand. Science. 2002;29(5565):151–5.
7. Allman R, Cowburn P, Mason M. In vitro and in vivo effects of a cyclic peptide with affinity for the $\alpha_v\beta_3$ integrin in human melanoma cells. Eur J Cancer. 2000;36(3):410–22.
8. Garanger E, Boturyn D, Dumy P. Tumor targeting with RGD peptide ligands-design of new molecular conjugates for imaging and therapy of cancers. Anticancer Agents Med Chem. 2007;7(5):552–8.
9. Welsh D, Smith D. Comparing dendritic and self-assembly strategies to multivalency-RGD peptide-integrin interactions. Org Biomol Chem. 2011;9(13):4795–801.
10. Miyamoto S, Akiyama S, Yamada K. Synergistic roles for receptor occupancy and aggregation in integrin transmembrane function. Science. 1995;267(5199):883–5.
11. Danhier F, Vroman B, Lecouturier N, Crokart N, Pourcelle V, Freichels H, *et al.* Targeting of tumor endothelium by RGD-grafted PLGA-nanoparticles loaded with paclitaxel. J Control Release. 2009;140(2):166–73.
12. Danhier F, Lecouturier N, Vroman B, Jérôme C, Marchand-Brynaert J, Feron O, *et al.* Paclitaxel-loaded PEGylated PLGA-based nanoparticles: In vitro and in vivo evaluation. J Control Release. 2009;133(1):11–7.
13. Wang Y, Wang X, Zhang Y, Yang S, Wang J, Zhang X, *et al.* RGD-modified polymeric micelles as potential carriers for targeted delivery to integrin-overexpressing tumor vasculature and tumor cells. J Drug Target. 2009;17(6):459–67.
14. Nasongkla N, Shuai X, Ai H, Weinberg B, Pink J, Boothman D, *et al.* cRGD-functionalized polymer micelles for targeted doxorubicin delivery. Angew Chem Int Ed Engl. 2004;43(46):6323–7.
15. Hartgerink J, Beniash E, Stupp SI. Peptide-amphiphilenanofibers: a versatile scaffold for the preparation of self-assembling materials. Proc Natl Acad Sci U S A. 2002;99(8):5133–8.
16. Accardo A, Tesauro D, Mangiapia G, Pedone C, Morelli G. Nanostructures by self-assembling peptide amphiphile as potential selective drug carriers. Biopolymers. 2007;88(2):115–21.
17. Cui H, Webber M, Stupp SI. Self-assembly of peptide amphiphiles: from molecules to nanostructures to biomaterials. Biopolymers. 2010;94(1):1–18.
18. Javali N, Raj A, Saraf P, Li X, Jasti B. Fatty acid - RGD peptide amphiphile micelles as potential paclitaxel delivery carriers to $\alpha_v\beta_3$ integrin overexpressing tumors. Pharm Res. 2012;29(12):3347–61.
19. Shen S, Kotamraj P, Bhattacharya S, Li X, Jasti B. Synthesis and characterization of RGD-fatty acid amphiphilic micelles as targeted delivery carriers for anticancer agents. J Drug Target. 2007;15(1):51–8.
20. McCusker B, Kocienski P, Boyle T, Schatzlein A. Solid-phase synthesis of c(RGDfK) derivatives: on-resin cyclisation and lysine functionalisation. Bioorg Med Chem Lett. 2002;12(4):547–9.
21. Wang W, Wu Q, Pasuelo M, McMurray J, Li C. Probing for integrin $\alpha_v\beta_3$ binding of RGD peptides using fluorescence polarization. Bioconjug Chem. 2005;16(3):729–34.
22. Raj A, Saraf P, Javali N, Li X, Jasti B. Binding and uptake of novel RGD micelles to the $\alpha v\beta 3$ integrin receptor for targeted drug delivery. J Drug Target. 2014;22(6):518–27.
23. Mas-Moruno C, Rechenmacher F, Kessler H. Cilengitide: the first anti-angiogenic small molecule drug candidate. design, synthesis and clinical evaluation. anticancer agents. Med Chem. 2010;10(10):753–68.
24. Sezgin Z, Yuksen N, Baykara T. Preparation and characterization of polymeric micelles for solubilization of poorly soluble anticancer drugs. Eur J Pharm Biopharm. 2006;64(3):261–8.
25. Tummino PJ, Gafni A. Determination of the aggregation number of detergent micelles using steady-state fluorescence quenching. Biophys J. 1993;64(5):1580–7.
26. Missirlis D, Farine M, Kastantin M, Ananthanarayanan B, Neumann T, Tirell M. Linker chemistry determines secondary structure of p53(14–29) in peptide amphiphile micelles. Bioconjugate Chem. 2010;21(3):465–75.
27. Lu J, Owen S, Stoichet M. Stability of self-assembled polymeric micelles in serum. Macromolecules. 2011;44(15):6002–8.
28. Chen CL, Hou WH, Liu IH, Hsiao G, Huang SS, Huang JS. Inhibitors of clathrin-dependent endocytosis enhance TGFβ signaling and responses. J Cell Sci. 2009;122(Pt 11):1863–71.
29. Shin S., Wolgamott L., Yoon S., Integrin trafficking and tumor progression, Int J Cell Biol., 2012; 2012: Article ID: 516789.
30. McMahon H, Boucrot E. Molecular mechanism and physiological functions of clathrin-mediated endocytosis. Nat Rev Mol Cell Biol. 2011;12:517–33.
31. Raymond E, Hanauske A, Faivre S, Izbicka E, Clark G, Rowinsky EK, *et al.* Effects of prolonged versus short-term exposure paclitaxel (Taxol) on human tumor colony-forming units. Anticancer Drugs. 1997;8(4):379–85.
32. Cai LL, Liu P, Li X, Huang X, Ye YQ, Chen FY, *et al.* RGD peptide-mediated chitosan-based polymeric micelles targeting delivery for integrin-overexpressing tumor cells. Int J Nanomedicine. 2011;6:3499–508.
33. Zhang L, He Y, Ma G, Song C, Son H. Paclitaxel-loaded polymeric micelles based on poly(ε-caprolactone)-poly(ethylene glycol)-poly(ε-caprolactone) triblockcopolymers:in vitro and in vivo evaluation. Nanomedicine. 2012;8(6):925–34.